Assessing bioorganic gum performance as a corrosion inhibitor in phosphoric acid medium: Electrochemical and computational analysis

Article *in* Materials and Corrosion · October 2021

DOI: 10.1002/maco.202112742

CITATIONS
0

READS
128

7 authors, including:

Sathiyapriya Thangavel
Dr. Mahalingam College of Engineering and Technology
16 PUBLICATIONS **30** CITATIONS
SEE PROFILE

Manikandan Dhayalan
Anticancer bioscience
10 PUBLICATIONS **6** CITATIONS
SEE PROFILE

Su MOHAMMED Riyaz
Islamiah College
3 PUBLICATIONS **0** CITATIONS
SEE PROFILE

Moonis Ali Khan
King Saud University
181 PUBLICATIONS **4,284** CITATIONS
SEE PROFILE

Received: 18 August 2021 | Accepted: 2 October 2021

DOI: 10.1002/maco.202112742

ARTICLE

Materials and Corrosion

Assessing bioorganic gum performance as a corrosion inhibitor in phosphoric acid medium: Electrochemical and computational analysis

Sathiyapriya T.[1] | **Manikandan Dhayalan**[1] | **Jagadeeswari R.**[2] | **Rathika Govindasamy**[3] | **Mohammed Riyaz S. U.**[4] | **Moonis Ali Khan**[5] | **Mika Sillanpää**[6]

[1]Department of Chemistry, Dr. Mahalingam College of Engineering and Technology, Coimbatore, Tamil Nadu, India

[2]Department of Chemistry, KPR Institute of Engineering and Technology, Coimbatore, Tamil Nadu, India

[3]Department of Chemistry, PSG College of Arts and Science, Coimbatore, Tamil nadu, India

[4]Molecular Biology Unit, PG & Research Department of Biotechnology, Islamiah College, Vaniyambadi, Tamil Nadu, India

[5]Chemistry Department, College of Science, King Saud University, Riyadh, Saudi Arabia

[6]Environmental Engineering and Management Research Group, Ton Duc Thang University, Ho Chi Minh City, Vietnam

Correspondence
T. Sathiyapriya, Department of Chemistry, Dr. Mahalingam College of Engineering and Technology, Coimbatore 642 003, India.
Email: sathiyachallenge87@gmail.com

Funding information
Researchers Supporting Project, Grant/Award Number: RSP-2021/345

Abstract

The present investigation was aimed at exploring the anticorrosive behavior of bio-organic *Auraucaria heterophylla* gum exudate (AHGE) on mild steel (MS) corrosion in 1 M phosphoric acid solution by weight loss technique, electrochemical studies, and computational analysis. Additionally, the performance was analyzed by morphological and quantum chemical analyses. The weight loss data revealed that AHGE showed 80% of inhibition efficiency at 303 K temperature. Inhibitor adsorption on MS was in line with Langmuir and Tempkin adsorption isotherms. Potentiodynamic studies showed that the investigated AHGE performed as a mixed-type inhibitor. Electrochemical parameters like charge transfer resistance, double-layer capacitance, and inhibition efficiency were determined and presented. Results obtained through computational analysis, scanning electron microscopy/energy dispersive X-ray analysis, and atomic force microscopy studies were well supported by the inhibitive potential of AHGE.

KEYWORDS
acid medium, computational analysis, corrosion, electrochemical studies, mild steel

1 | INTRODUCTION

Corrosion can be popularly pronounced as a deteriorative loss of a metal as a consequence of dissolution due to chemical or electrochemical reactions. Mild steel (MS) is one of the most familiar metals engaged broadly in a wide range of industries.[1–3] During a number of industrial procedures, acidic solutions are generally used for the elimination of impurities, rust, and others. However, the main problem of exposing MS in acidic

solutions is its dissolution. Hence, inhibitors are used during these processes to prevent metal deterioration/dissolution. The most commonly used acid inhibitors are N, O, and S containing organic and heterocyclic compounds with polar functional groups and conjugated double bonds.[4–8] Both natural and synthetic compounds may be frequently used as corrosion inhibitors. These compounds get adsorbed on metal surfaces and hinder the active corrosion sites formation, consequently protect the metal from deterioration. However, most of the synthetic corrosion inhibiting compounds are costly and found to be toxic to both living organisms and the environment. To address these critical concerns it is very important to develop cost-effective, nontoxic, and eco-friendly natural products as metal corrosion inhibitors.

Plant extracts are exceedingly a good source of corrosion inhibitors. A wide variety of plants including herbs, shrubs, trees, climbers, and creepers can be used for the corrosion inhibition process. They are extracted through simple cost-efficient steps. It was found that the extracts of *Tephrosia purpurea*,[9] *Houttuynia cordata*,[10] *Cassava* (*Manihot esculenta*),[11] *Kola nitida*,[12] coconut coir dust,[13] and *Aspilia africana*[14] contain a mixture of compounds that are proved to be valuable corrosion inhibitors. The present work is an attempt to explore the corrosion inhibition properties of gum exudate of *Araucaria heterophylla*, a member of Araucariaceae family on MS corrosion in 1 M phosphoric acid (H_3PO_4) medium.

2 | EXPERIMENTAL

2.1 | Sample preparation

MS specimens were cut into regular rectangular pieces of dimensions 5 × 1 cm and 2 mm thickness. Thereafter, the MS plates were degreased well with acetone, dried, polished well with various grade emery sheets to have a uniform smooth surface weighed and kept stored in a desiccator. The initial and final weights of the specimens were observed.

2.2 | Preparation of medium and plant extract

The blank corrosive acidic medium namely 1 M H_3PO_4 was prepared by diluting analytical reagent grade H_3PO_4 in deionized (D.I.) water. Gum exudate of *Araucaria heterophylla* (AHGE) was collected, cleaned, and washed well with D.I. water. Five grams of AHGE were dissolved in 500 ml of D.I. water to prepare a 1% stock solution. The stock solution was diluted with the appropriate quantity of 1 M H_3PO_4 to obtain inhibitor test solutions of varying concentrations.

2.3 | Weight loss analysis

For weight loss measurements, MS specimens were completely kept exposed in 100 ml test solution of the acidic environment (1 M H_3PO_4) in the absence and presence of the inhibitor at varied temperatures (303, 313, 323, and 343 K). From the weight loss of the MS, the corrosion rate (CR) was determined according to Reference Equation (1) [15] as:

$$\mathrm{CR(mpy)} = 534\,W/DAt, \tag{1}$$

where W is the weight loss (mg), D is the density of MS (7.8 g/cm^3), A is the area of the specimen (4.7244 in.^{2}), and t is the time of immersion (h).

The percentage inhibition efficiency (I.E.%) was calculated according to Equation (2) Reference [16] as:

$$\mathrm{I.\,E.\,\%} = \frac{W_o\text{-}W_i}{W_o} \times 100, \tag{2}$$

where W_o and W_i are the weight loss values in absence and presence of inhibitor, respectively.

2.4 | Electrochemical analysis

Electrochemical measurements were carried out in a typical three-electrode system. The platinum electrode as a counter electrode, saturated calomel as a reference electrode, and MS as working electrode were set at room temperature for the measurement. The potential range of −200 to +200 mV w.r.t to open circuit potential at a scan rate of 1 mV/s and a frequency range of 0.1 to 20 000 Hz with a signal amplitude of 10 mV in presence and absence of inhibitor in 1 M H_3PO_4 were maintained. From the Nyquist plot, various impedance parameters including charge transfer resistance (R_{ct}) and double-layer capacitance (C_{dl}) were calculated.[17] The I.E. I_{corr} and I.E.% were determined as follows:

$$I_{corr} = \frac{b_a \times b_c}{2.303(b_a + b_c)} \times \frac{1}{R_{ct}}, \tag{3}$$

where R_{ct} is the charge transfer resistance and b_a and b_c are the Tafel slopes.

Equation (3) is called Stern Geary Equation:

$$\text{I. E. \%} = \frac{I_{\text{corr}}(\text{blank}) - I_{\text{corr}}(\text{inh})}{I_{\text{corr}}(\text{blank})} \times 100, \quad (4)$$

where I_{corr}(blank) is the corrosion current without inhibitor and I_{corr} (inh) is the corrosion current with inhibitor and

$$\text{I. E. \%} = \frac{R_{\text{ct}}(\text{blank}) - R_{\text{ct}}(\text{inh})}{R_{\text{ct}}(\text{blank})} \times 100, \quad (5)$$

where R_{ct} (blank) is the charge transfer resistance without inhibitor and R_{ct} (inh) is the charge transfer resistance with inhibitor.

2.5 | Gas chromatography–mass spectroscopic (GC–MS) analysis

The GC–MS is one of the important and advanced tools used to identify the compounds present in the plant extract. The analysis was carried out using Shimadzu (GC-MS-QP2010 SE) instrument consisting of column Elite-1 fused silica capillary, functioning in electron impact mode at 70 eV. The carrier gas helium (99.999%) was preferred at a constant flow of 1 ml/min at injection temperature 280°C; ion-source temperature 200°C. The oven temperature was 100°C, maintained isothermally for 4 min, with a regular increase of 10°C/min, to 200°C, then 5°C/min to 270°C, ending with a 9-min isothermal at 270°C. The total GC working time was 53 min.[18]

2.6 | Scanning electron microscopy–energy dispersive X-ray (SEM-EDX) analysis

The surface morphology of MS specimens kept immersed in 1 M H_3PO_4 in the absence and presence of AHGE extract at room temperature for 3 h was performed using Carl Zeiss Evo18-make scanning electron microscope. The elemental composition of the sample was also examined by EDX analysis.[19]

2.7 | Atomic force microscopy (AFM)

The surface analysis of the MS was examined using AFM after 2 h immersion time at room temperature in the absence and presence of AHGE by NTEGRA Prima—AFM. After immersion, the MS was removed out of the solution, washed well without affecting the surface, and the properties were studied.[20]

2.8 | Quantum chemical approach

Quantum chemical observations were carried out with the aid of density functional theory (DFT). The electronic structure of AHGE on MS surface was exhibited by DFT/B3LYP/6-311 G (d,p) level of basis set using the Gaussian 09 program.[21] Among the compounds identified during GC–MS analysis cholest-14-ene and 1-ethenyl-1-methyl-2-(1-methylethenyl)-4-(1-methylethylidene) were selected which possess high peak area % and the quantum studies were carried out. All the quantum parameters were determined using B3LYP functional and a 6-3IG basis set.

3 | RESULTS AND DISCUSSION

3.1 | Weight loss measurement

3.1.1 | Effect of inhibitor concentration

Weight loss measurements of MS specimen was carried out at varied immersion time periods (1, 3, 5, 7, and 24 h) and various temperatures ranging from 303 to 333 K in 1 M H_3PO_4 medium in the absence and presence of inhibitor. During the studied time periods, the CR was found to decrease on increasing the inhibitor concentration, illustrated in Figure 1. This is attributed to the fact that the phytoconstituents of AHGE get adsorbed on to the MS surface. The CR and I.E. at varied temperatures are given in Table 1. It was found that a maximum I.E. of 95.56% was reached at 303 K temperature in presence of 0.05% v/v of inhibitor concentration. Thereafter, it decreases due to the desorption of AHGE molecules from the MS surface. In addition, it was found that the I.E. values showed an increment only up to 0.05% of AHGE concentration and after that significant increase in I.E. was not found. Hence, it was considered as an optimum inhibitor concentration for MS protection from corrosion. Variation in I.E. with the temperature at various concentrations of AHGE inhibitor is displayed in Figure 2. It was observed that I.E. increases on increasing the concentration of the inhibitor at all the studied temperatures. This is attributed to the adsorption of the AHGE molecules onto the surface of the MS and IE was found to decrease on increasing the temperature, which may be due to desorption of AHGE from the MS surface, an indicative of physical adsorption mechanism.[22–24]

3.1.2 | Adsorption isotherm

Adsorption isotherms are an important analytical tool, which helps in finding out the mode of adsorption of

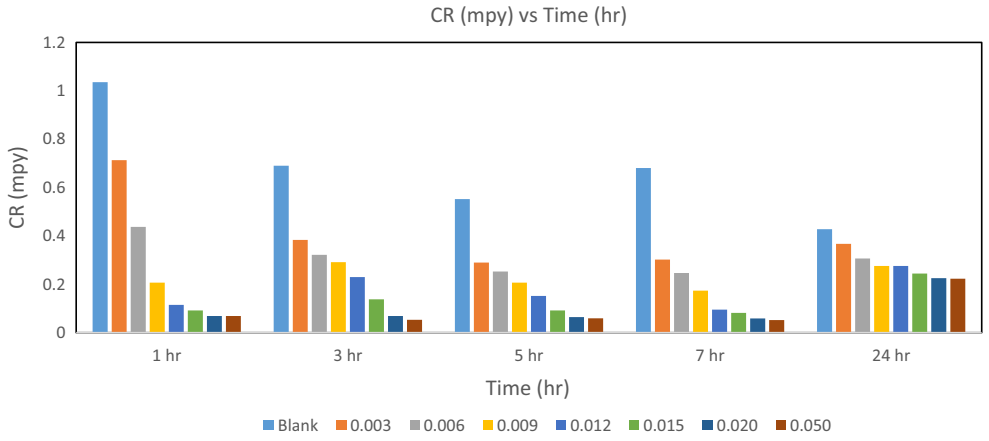

FIGURE 1 Effect of time on corrosion rate (CR) in presence and absence of *Araucaria heterophylla* gum exudate extract in 1 M H_3PO_4 medium [Color figure can be viewed at wileyonlinelibrary.com]

TABLE 1 CR and I.E. % of AHGE extract in 1 M H_3PO_4 at various concentrations and temperatures

		Temperature (K)							
		303		313		323		333	
S. no.	Inhibitor conc. % (v/v)	CR (mpy)	I.E. (%)	CR (mpy)	I.E. (%)	CR (mpy)	I.E. (%)	CR (mpy)	I.E. (%)
1.	Blank	1.036		1.7267		2.348		3.246	
2.	0.003	0.4144	60.00	0.7367	57.33	1.3353	43.14	1.8648	42.55
3.	0.009	0.2072	80.00	0.5295	69.33	0.9669	58.82	1.5885	51.06
4.	0.015	0.0921	91.11	0.3453	80.00	0.7367	68.63	1.2662	60.99
5.	0.020	0.0691	93.33	0.2763	84.00	0.5756	75.49	1.0360	68.09
6.	0.050	0.0460	95.56	0.2532	85.33	0.5986	74.51	0.9209	71.63

Abbreviations: AHGE, *Araucaria heterophylla* gum exudate; CR, corrosion rate; I.E., inhibition efficiency; mpy, miles per year.

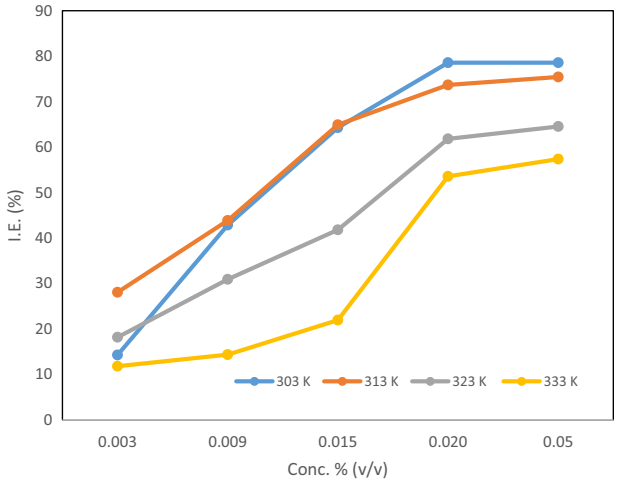

FIGURE 2 Effect of inhibitor concentration on inhibition efficiency in 1 M H_3PO_4 medium [Color figure can be viewed at wileyonlinelibrary.com]

AHGE molecules on the MS surface.[25] The surface coverage (Θ) values determined through gravimetric measurements at varied concentrations of the inhibitor for temperature range 303–333 K were fitted to different adsorption isotherms. It was found that the best fits were obtained for both Langmuir and Temkin adsorption isotherms (Figures 3 and 4) with regression coefficient (R^2) values close to unity. This suggests a mixed-type inhibition mechanism. The surface coverage values fit well to the Langmuir adsorption isotherm. This shows that the organic compounds containing polar atoms present in AHGE get adsorbed on the MS by mutual repulsion or attraction which in turn implies monolayer adsorption of inhibitor.[26] Temkin adsorption isotherm suggests the presence of attractive force exists between MS surface and the inhibitor responsible for improved inhibition and also attributed to the fact that each active site of the metal surface is occupied by inhibitor molecule.[27]

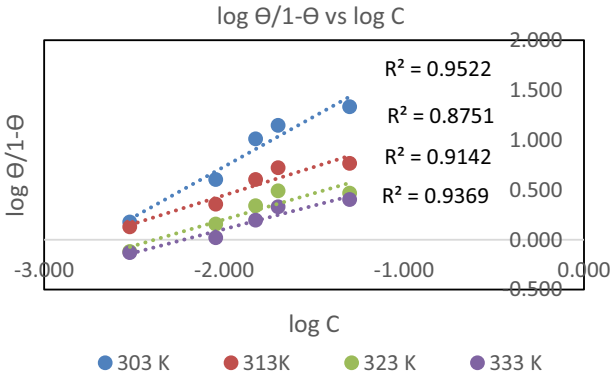

FIGURE 3 Langmuir adsorption isotherm [Color figure can be viewed at wileyonlinelibrary.com]

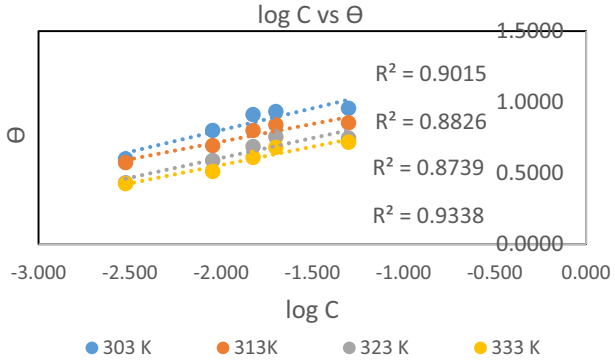

FIGURE 4 Tempkin adsorption isotherm [Color figure can be viewed at wileyonlinelibrary.com]

3.2 | Electrochemical measurements

3.2.1 | Potentiodynamic polarization technique

Tafel plot of MS specimen in 1 M H_3PO_4 medium in the absence and presence of AHGE is displayed in Figure 5. Potentiodynamic polarization parameters like corrosion potential (E_{corr}), corrosion current density (I_{corr}), Tafel slopes (β_a and β_c) and polarization resistance (R_p) are given in Table 2. It can be concluded from the data presented in Table 2 that I_{corr} values show a predominant decrease with an increase in the concentration of the AHGE inhibitor. This establishes the formation of a protective layer of AHGE over MS surface.[28,29] It was also found that the E_{corr} values do not show a substantial change suggesting the inhibitor as mixed-type. The Tafel slope values also show changes compared to blank. This indicates that both anodic and cathodic reactions were delayed after the addition of inhibitors.[30] The R_p values were found to increase on increasing the concentration of the inhibitor. I.E. were calculated using R_p values and it was found that the I.E. increases on increasing the inhibitor concentration in the acid medium.[31,32]

3.2.2 | Electrochemical impedance technique

Figure 6 illustrates the Nyquist plot in the absence and presence of inhibitors in 1 M H_3PO_4 solution.

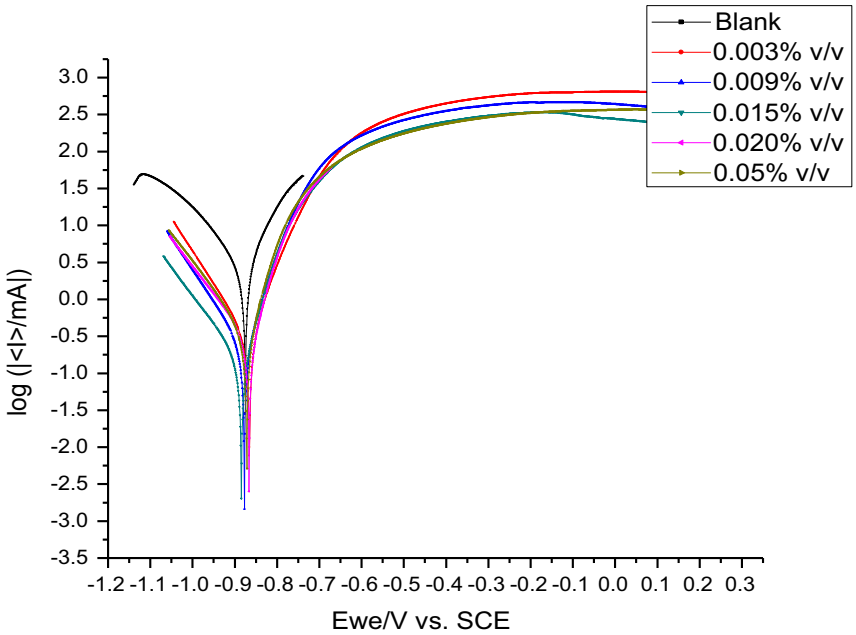

FIGURE 5 Potentiodynamic polarization curves for mild steel in 1 M H_3PO_4 containing varied concentrations of *Araucaria heterophylla* gum exudate inhibitor [Color figure can be viewed at wileyonlinelibrary.com]

TABLE 2 Kinetic and impedance parameters of mild steel in 1 M H_3PO_4 containing varied concentrations of *Araucaria heterophylla* gum exudate

S. no.	Inhibitor conc. (% v/v)	$-E_{corr}$ (mV)	I_{corr} (μA)	β_a (mV/dec)	β_c (mV/dec)	R_p ($\Omega\,cm^2$)	I.E. (%)	
							I_{corr}	R_p
1	Blank	884.17	822.45	111	174.4	358.11	–	–
2	0.003	869.48	644.21	120	128.1	417.62	21.67	14.25
3	0.009	893.87	436.19	77.2	132.7	485.85	46.96	26.29
4	0.015	881.45	272.69	70.1	97.1	648.25	66.84	44.76
5	0.02	880.22	249.16	93.3	162.9	1033.83	69.7	65.36
6	0.05	888.27	209	76.2	147.1	1042.89	74.59	65.66

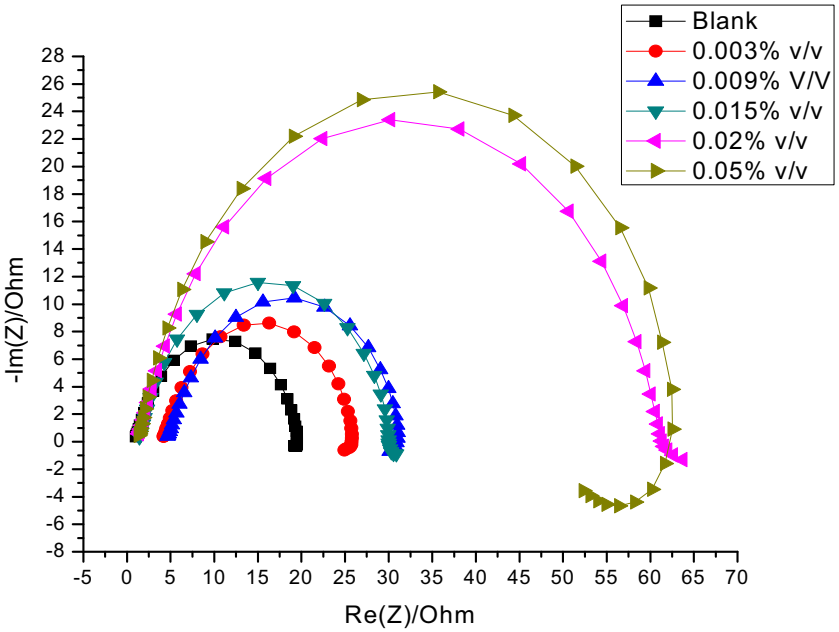

FIGURE 6 Nyquist plot of mild steel in 1 M H_3PO_4 in the absence and presence of various concentrations of *Araucaria heterophylla* gum exudate inhibitor [Color figure can be viewed at wileyonlinelibrary.com]

TABLE 3 Impedance parameters for mild steel in 1 M H_3PO_4 in the absence and presence of various concentrations of inhibitor

S. no.	Inhibitor conc. (% v/v)	R_{ct} (Ω)	C_{dl} (F)	I.E.%	
				C_{dl}	R_{ct}
1.	Blank	19.294	1.254×10^{-4}	–	–
2.	0.003	23.045	91.23×10^{-6}	27.48	16.28
3.	0.009	33.05	79.52×10^{-6}	36.79	41.62
4.	0.015	33.75	38.87×10^{-6}	69.10	42.83
5.	0.02	63.92	25.25×10^{-6}	79.71	69.82
6.	0.05	65.25	18.25×10^{-6}	85.49	70.43

Abbreviations: C_{dl}, double-layer capacitance; I.E.%, percentage inhibition efficiency; R_{ct}, charge transfer resistance.

Electrochemical impedance parameters like R_{ct} and C_{dl} are given in Table 3. It can be observed that the C_{dl} value for an uninhibited solution was comparatively higher than for inhibited solution, owing to the decreased dielectric constant and increased electrical double-layer capacitance. It could be identified that the R_{ct} values were found to increase on increasing the concentration of AHGE. This may be recognized as to decrease in local dielectric constant or an increase in thickness of the electrical double layer. I.E.s were calculated using C_{dl} and R_{ct} values. It was found that the I.E.% increases on increasing the inhibitor concentration in the acid medium.[33–36]

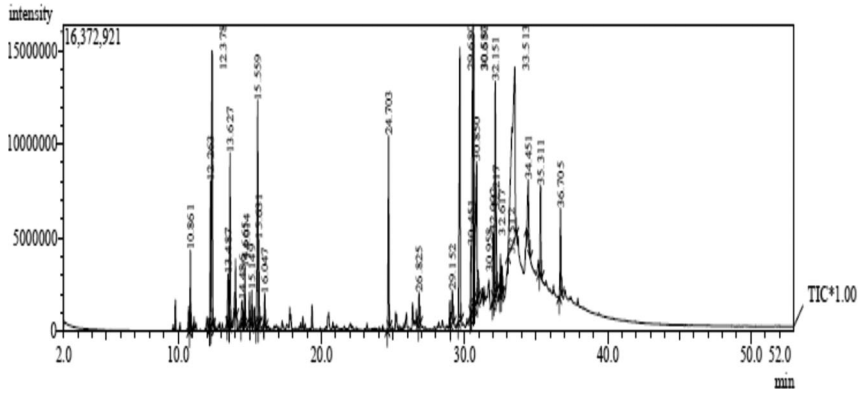

FIGURE 7 Gas chromatography–mass spectroscopic spectrum of *Araucaria heterophylla* gum exudate

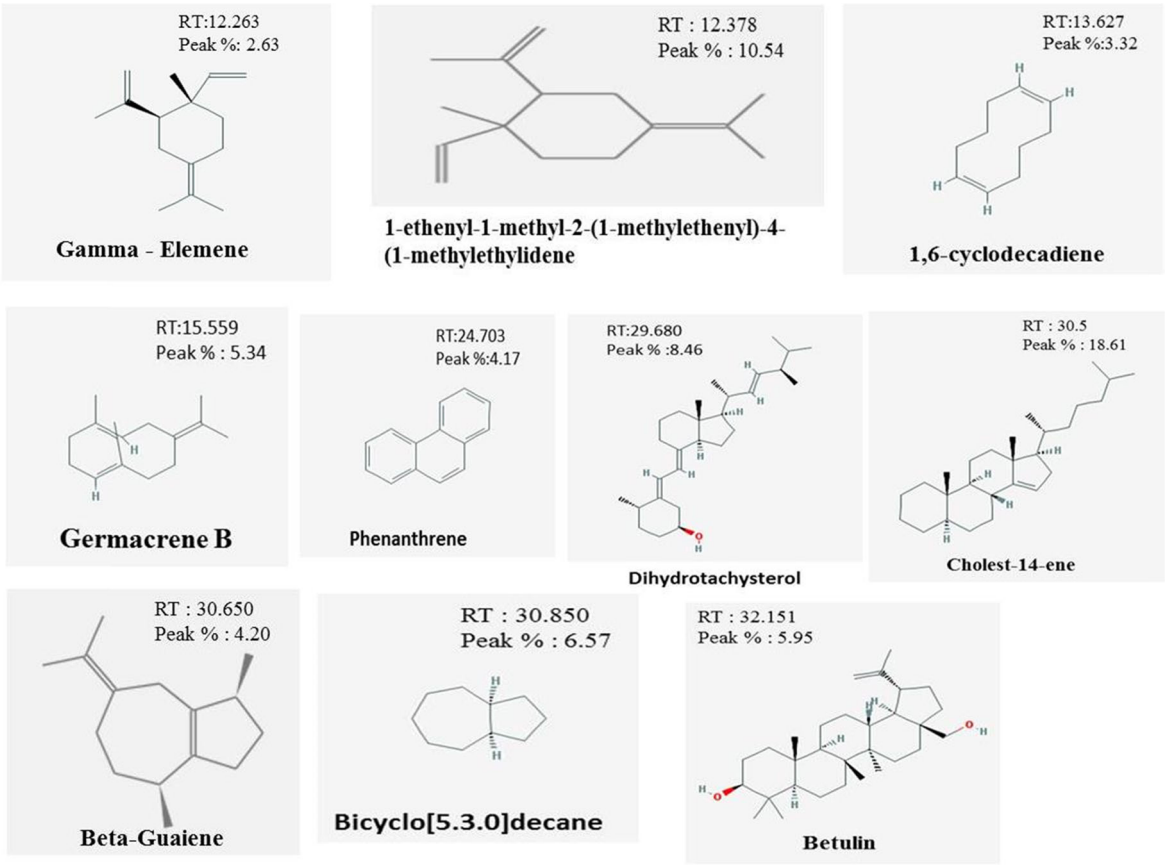

FIGURE 8 Chemical structures of compounds identified in *Araucaria heterophylla* gum exudate [Color figure can be viewed at wileyonlinelibrary.com]

3.3 | GC–MS analysis

Figure 7 displayed the GC–MS spectrum of AHGE. Chemical structures of the compounds (having high area percentage) identified from the GC–MS spectra of AHGE are presented in Figure 8. From the list of compounds identified cholest-14-ene and 1-ethenyl-1-methyl-2-(1-methylethenyl)-4-(1-methylidene) were selected. Owing to their excellent peak percentage and retention time the quantum chemical analysis was carried out.

3.4 | Computation analysis

3.4.1 | Quantum chemical studies

The optimized structures of cholest-14-ene and 1-ethenyl-1-methyl-2-(1-methylethenyl)-4-(1-methylidene) are presented in Figure 9a,b, and the calculated quantum chemical parameters are given in Table 4. Highest occupied molecular orbital (HOMO) and lowest occupied molecular orbital (LUMO) images for the compound A and B are illustrated in

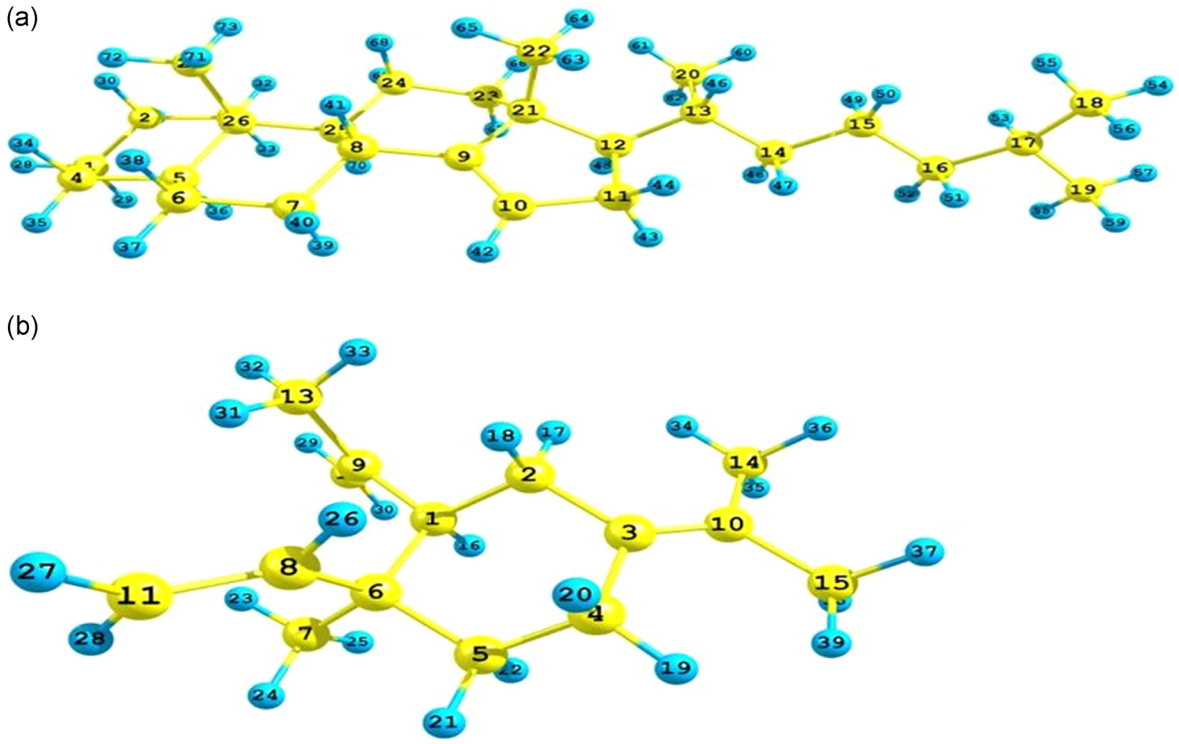

FIGURE 9 Optimized structures of (a) cholest-14-ene (compound A) and (b) 1-ethenyl-1-methyl-2-(1-methylethenyl)-4-(1-methylidene) (compound B) [Color figure can be viewed at wileyonlinelibrary.com]

TABLE 4 Quantum chemical parameters

S. no.	Quantum descriptor	Cholest-14-ene (compound A)	1-eEthenyl-1-methyl-2-(1-methylethenyl)-4-(1-methylidene) (compound B)
1.	E_{HOMO} (eV)	−6.0023	−5.887
2.	E_{LUMO} (eV)	0.9137	0.5175
3.	ΔE (eV)	6.91	6.405
4.	Dipole moment (μ)	0.3909	0.6083
5.	Ionization energy (I)	6.0023	5.887
6.	Electronic affinity (A)	−0.9137	−0.5175
7.	Electronegativity (χ)	2.5443	2.6848
8.	Global hardness (η)	3.458	3.2023
9.	Global softness (S)	0.2892	0.3123
10.	Fraction of electrons transferred (ΔN)	0.6442	0.6738
11.	Electrophilicity index (ω)	0.9360	0.4192
12.	Chemical potential	−2.5443	−2.6848

Abbreviations: HOMO, highest occupied molecular orbital; LUMO, lowest occupied molecular orbital.

Figure 10a,b. E_{HOMO} values are related to the electron-donating ability of a molecule. E_{LUMO} values are associated with the electron-accepting ability of a molecule. Higher E_{HOMO} and lower E_{LUMO} values facilitate a higher tendency to transfer its electrons to the suitable unoccupied d-orbitals of the MS and simultaneously accept the electrons from the MS which enables better adsorption, followed by increased I.E. and more likely to accept electrons, respectively.[37]

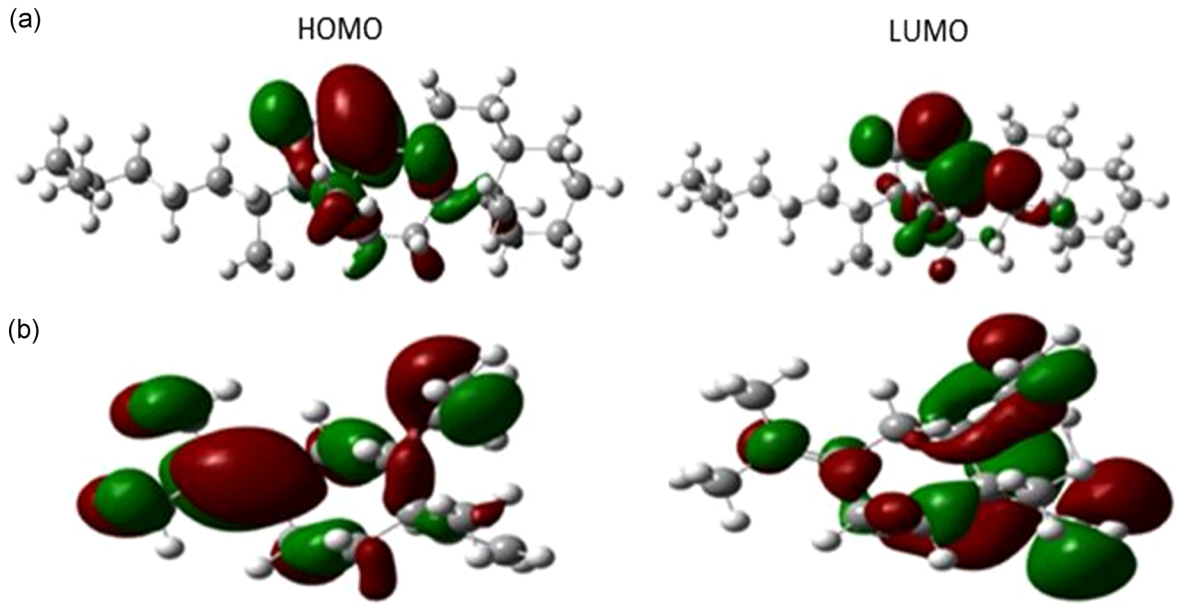

FIGURE 10 Highest occupied molecular orbital (HOMO) and lowest occupied molecular orbital (LUMO) images of (a) compound A and (b) compound B [Color figure can be viewed at wileyonlinelibrary.com]

Energy gap $(\Delta E) = E_{LUMO} - E_{HOMO}$, low values of ΔE gives predominant I.E., as the energy required to take out an electron from the last occupied orbital will be least. On comparing the ΔE values of compounds A and B it was found that that compound B possesses a low energy gap and hence compound B may support the corrosion inhibition process more effectively than compound A, obviously giving high I.E.[38] Chemical reactivity of the atoms and molecules of the organic compounds A and B were described with the help of another parameter called ionization energy (I), which is the amount of energy essential to remove electrons from a molecule. It is said that compounds having low ionization energy are efficient in corrosion inhibition, as it helps for the good reactivity of atoms and molecules with the MS surface. In that aspect, the I values of compounds A and B were compared and it was found that compound B had low I values. It indicates the high reactivity of the atoms towards the MS surface.

Other parameters like electronegativity (χ), global hardness (η), and softness (S) are correlated with the stability and reactivity of the inhibitor molecule. Chemical hardness describes the resistance towards the deformation or electron cloud polarization of chemical species, it is further specified that hard molecules possess a large energy gap, implying low polarizability. Hard molecules are considered to be less active than soft molecules, as a result, electrons may be offered to another molecule more easily. Hence in a rusting process, MS is deliberated as soft acid and will coordinate with molecules possessing high softness. In this aspect, compound B exhibited a higher softness value than compound A. This facilitates better adsorption on the MS surface.[39–41]

Dipole moment (μ) is another more pronounced parameter, which foretells the pathway of the corrosion inhibition process. It is generally agreed that the compounds possessing high μ indicate the stability of the inhibitor. This results in achieving better corrosion inhibition. In the present work, compound B possesses a higher μ value than compound A, this indicates a high I.E.[42] Electrophilicity (ω) data gives detailed information about the electrophilic or nucleophilic nature of the molecule. Molecules with high electrophilic value acquires the capacity to act as an electrophile, while a low electrophilicity value notifies that the molecule has a high tendency to act as a nucleophile. In the present study, ω value for compound A was greater than compound B. The fraction of electrons transferred (ΔN) is the ability of the molecule to donate electrons to adhere on to the surface of the MS specimen. Higher ΔN values increase the electron-donating ability of the inhibitor to the metal surface, hence increase the corrosion I.E. In the present study, compound B possesses higher ΔN value compared to compound A.[43,44] On analyzing all the aspects it was concluded that compound B supports the corrosion inhibition process more effectively than compound A.

3.5 | Surface morphology

3.5.1 | SEM analysis

Figure 11a,b display SEM images of MS immersed in 1 M H_3PO_4 in the absence and presence of AHGE after 3 h

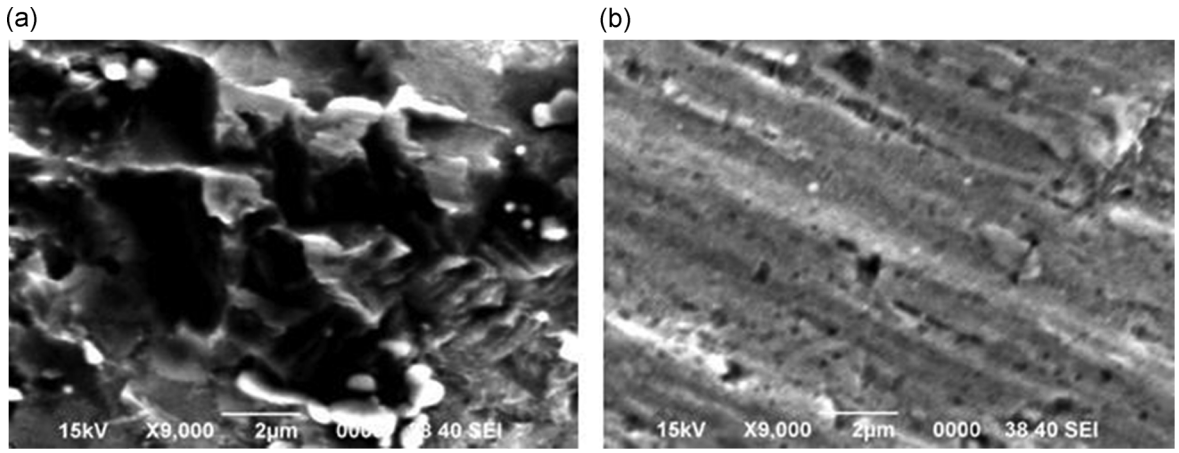

FIGURE 11 Surface morphology of mild steel immersed in 1 M H_3PO_4 in (a) absence and (b) presence of *Auraucaria heterophylla* gum exudate

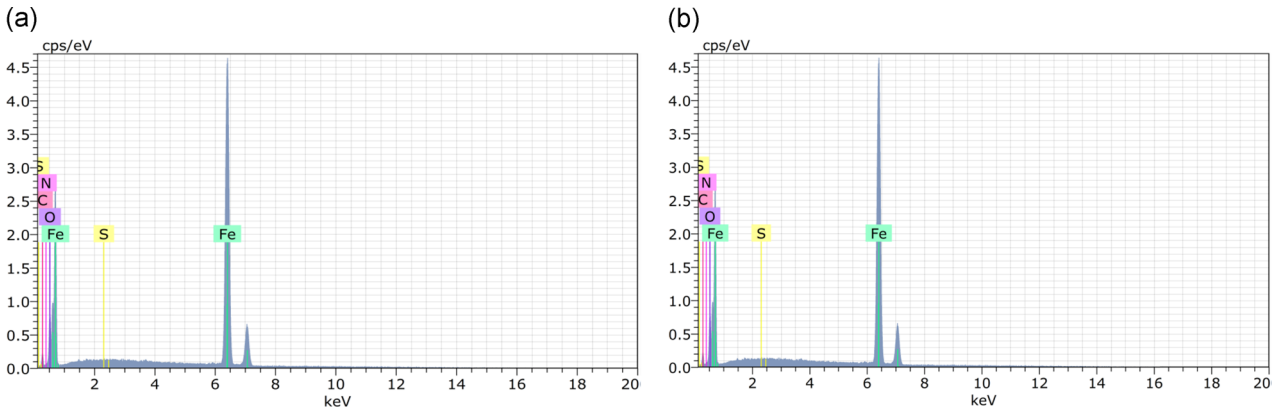

FIGURE 12 Energy dispersive X-ray spectrum of mild steel (a) without and (b) with inhibitor [Color figure can be viewed at wileyonlinelibrary.com]

TABLE 5 Elemental weight percentage obtained from energy dispersive X-ray spectra

S. no.	Treatment	Content elements (wt%)		
		Fe	O	C
1.	Mild steel without inhibitor	67.23	20.16	7.05
2.	Mild steel with inhibitor	81.59	14.06	11.02

immersion. It was found that the MS specimen aggressively corroded in the blank acid medium, displayed in Figure 11a. Figure 11b exhibits a smoother MS surface which is familiar to the fact that the inhibitor molecules get strongly adhered over the MS surface, thus, forming a protective film to inhibit corrosion.[45,46]

3.5.2 | EDX spectral analysis

EDX spectral images of MS plates without and with an inhibitor in the acid medium after immersion of 2 h are shown in Figure 12a,b. Elemental percentage of Fe, O, and C in MS in the absence and presence of inhibitor (AHGE) is given in Table 5. The elemental weight percentage of Fe increases significantly from 67.23% to 81.59%, while C increases from 7.05% to 11.02%. Thus, the formation of a protective barrier on the MS specimen was concluded. The decreased O percentage proves the formation of the passive layer on the MS surface by AHGE.[47,48]

3.5.3 | AFM analysis

Atomic force microscopy images of the MS specimen kept immersed in 1 M H_3PO_4 medium in the absence and

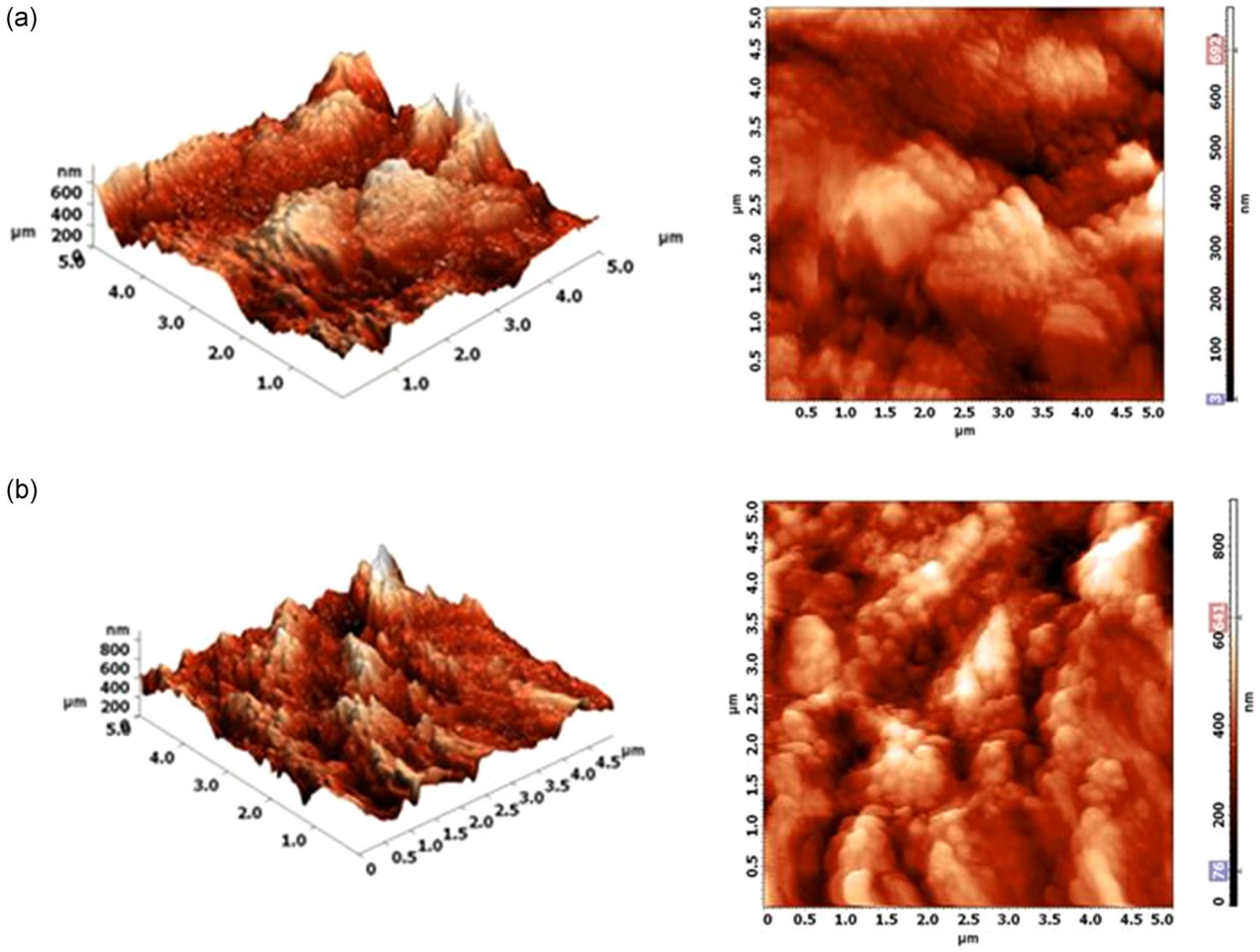

FIGURE 13 Three-dimensional and two-dimensional atomic force microscopy image of mild steel (a) without and (b) with *Auraucaria heterophylla* gum exudate inhibitor in 1 M H_3PO_4 medium [Color figure can be viewed at wileyonlinelibrary.com]

presence of inhibitor were taken to investigate the nature of the protective barrier layer formed on the surface of the MS specimen. The two-dimensional and three-dimensional images are displayed in Figure 13a,b. The average roughness for the MS sample immersed in acid medium in the absence and presence of inhibitor were 130.25 and 71.00 nm, respectively. The reduction in the roughness confirmed the adsorption of AHGE molecules on the MS surface.[49,50]

4 | CONCLUSIONS

Experimental and computational analyses were engaged to explore the corrosion protection tendency of AHGE on MS surface in a 1 M H_3PO_4 medium. Mass loss measurements showed that the I.E.% increases on increasing the inhibitor concentration and decreases on increasing the temperature. Electrochemical measurements showed that the inhibitor was mixed type and the inhibition process takes place by the adsorption of the inhibitor on the MS surface. The surface morphology studies (SEM-EDX and AFM) suggest the formation of the adsorbed protective layer on the MS which shows the efficiency of the AHGE. DFT studies were carried out for two compounds having a high peak pecentage present in AHGE. Both the experimental and computational analyses data were in good agreement.

ACKNOWLEDGMENTS

The authors gratefully acknowledges PSG College of Arts and Science, Coimbatore, Tamilnadu, India for rendering lab facility to carry out the work. The authors gratefully acknowledge Dr. M. Dhandapani, Associate Professor, Department of Chemistry, Sri Ramakrishna Mission Vidyalaya College of Arts and Science, Coimbatore, Tamilnadu, India for the support provided by him to proceed with DFT studies using Gaussian 09 software. Moonis Ali Khan acknowledges the financial support through Researchers Supporting Project number (RSP-2021/345), King Saud University, Riyadh, Saudi Arabia.

CONFLICT OF INTERESTS

The authors declare that there are no conflict of interests.

DATA AVAILABILITY STATEMENT

Research data are not shared.

ORCID

Sathiyapriya T. http://orcid.org/0000-0003-2798-3441

REFERENCES

[1] M. Chigondo, F. Chigondo, *J. Chem.* **2016**. *2016*, 7.
[2] N. I. N. Hais, S. Sobri, N. Kassim, *Mater. Corros.* **2019**, *70*, 1111.
[3] A. Saxena, D. Prasad, R. Haldhar, G. Singh, A. Kumar, *Mol. Liq.* **2018**, *258*, 89.
[4] V. Thailan, *Asian J. Chem.* **2020**, *32*, 395.
[5] R. Herle, S. Divakara Shetty, U. Achutha Kini, P. Shetty, *Chem. Eng. Commun.* **2011**, *198*, 120.
[6] S. Sharma, A. Kumar, *J. Mol. Liq.* **2021**, *322*, 114862.
[7] A.M. Al-Fakih, H. H. Abdallah, M. Aziz, *Mater. Corros.* **2019**, *70*, 135.
[8] S. Echihi, N. Benzbiria, M. E. Belghiti, M. El Fal, M. Boudalia, E. M. Essassi, A. Guenbour, A. Bellaouchou, M. Tabyaoui, M. Azzi, *Mater. Today: Proc.* **2021**, *37*, 3958.
[9] B. Thirumangalam Karunanithi, J. Chellappa, *J. Dispersion Sci. Technol.* **2019**, *40*, 1441.
[10] X. Zheng, M. Gong, Q. Li, *Int. J. Electrochem. Sci.* **2017**, *12*, 6232.
[11] D. R. Gusti, E. Admin Alif, M. Efdi, *Int. J. Chem. Technol. Res.* **2017**, *10*, 163.
[12] D. I. Njoku, I. Ukaga, O. B. Ikenna, E. E. Oguzie, K. L. Oguzie, N. Ibisi, *J. Mol. Liq.* **2016**, *219*, 417.
[13] S. A. Umoren, M. M. Solomon, U. M. Eduok, I. B. Obot, A. U. Israel, *J. Environ. Chem. Eng.* **2014**, *2*, 1048.
[14] I. M. Mejeha, M. C. Nwandu, K. B. Okeoma, L. A. Nnanna, M. A. Chidiebere, F. C. Eze, E. E. Oguzie, *J. Mater. Sci.* **2012**, *47*, 2559.
[15] S. Caprarescu, C. Modrogan, V. Purcar, A. Madelene Dancila, R. Claudiu Fierascu, *Rev. Chim.* **2019**, *70*, 1140.
[16] A. A.- Dawsari, A. M. Turkustani, F. Bannani, *J. Mater. Environ. Sci.* **2019**, *10*, 1135.
[17] A. Rodríguez-Torres, M. G. Valladares-Cisneros, C. Cuevas-Arteaga, M. A. Veloz-Rodríguez, *J. Mater. Environ. Sci.* **2019**, *10*, 101.
[18] A. Garaya, W. Dhifi, M. Nehiri, A. Echchelh, M. Ebntouhami, A. Chaouch, W. Mnif, R. Ben Chaouacha-Chekir, *J. New Sci.* **2016**, *30*, 1719.
[19] M. H. Hussin, M. J. Kassim, *J. Phys. Sci.* **2010**, *21*, 1.
[20] Q. A. Yousif, A. A. Al-Zhara, *J. Eng. Appl. Sci.* **2016**, *11*, 12619.
[21] Gaussian 09, Revision E.01, M. J. Frisch, G. W. Trucks, H. B. Schlegel, G. E. Scuseria, M. A. Robb, J. R. Cheeseman, G. Scalmani, V. Barone, B. Mennucci, G. A. Petersson, H. Nakatsuji, M. Caricato, X. Li, H. P. Hratchian, A. F. Izmaylov, J. Bloino, G. Zheng, J. L. Sonnenberg, M. Hada, M. Ehara, K. Toyota, R. Fukuda, J. Hasegawa, M. Ishida, T. Nakajima, Y. Honda, O. Kitao, H. Nakai, T. Vreven, J. A. Montgomery, Jr., J. E. Peralta, F. Ogliaro, M. Bearpark, J. J. Heyd, E. Brothers, K. N. Kudin, V. N. Staroverov, R. Kobayashi, J. Normand, K. Raghavachari, A. Rendell, J. C. Burant, S. S. Iyengar, J. Tomasi, M. Cossi, N. Rega, J. M. Millam, M. Klene, J. E. Knox, J. B. Cross, V. Bakken, C. Adamo, J. Jaramillo, R. Gomperts, R. E. Stratmann, O. Yazyev, A. J. Austin, R. Cammi, C. Pomelli, J. W. Ochterski, R. L. Martin, K. Morokuma, V. G. Zakrzewski, G. A. Voth, P. Salvador, J. J. Dannenberg, S. Dapprich, A. D. Daniels, O. Farkas, J. B. Foresman, J. V. Ortiz, J. Cioslowski, D. J. Fox Gaussian Inc., Wallingford CT **2009**.
[22] K. Krishnaveni, J. Ravichandran, *Trans. Nonferrous Met. Soc. China* **2014**, *24*, 2704.
[23] S. Manimegalai, P. Manjula, *J. Mater. Environ. Sci.* **2015**, *6*, 1629.
[24] A. Hamdy, N. S. El-Gendy, *Egypt. J. Pet.* **2013**, *22*, 17.
[25] R. Karthikaiselvi, S. Subhashini, *J. Assoc. Arab Univ. Basic Appl. Sci.* **2014**, *16*, 74.
[26] M. T. G. de Sampaio, C. Machado Fernandes, G. G. P. de Souza, E. S. Carvalho, J. A. C. Velasco, J. César, M. Silva, O. C. Alves, E. A. Ponzio, *J. Bio- Tribo-Corros.* **2021**, *7*, 14.
[27] L. H. Madkour, S. K. Elroby, *Int. J. Ind. Chem.* **2015**, *6*, 165.
[28] R. Haldhar, D. Prasad, A. Saxena, P. Singh, *Mater. Chem. Front.* **2018**, *2*, 1225.
[29] C. Verma, M. A. Quraishi, N. Kumar Gupta, *Ain Shams Eng. J.* **2018**, *9*, 1225.
[30] T. K. Chaitra, K. N. Mohana, D. M. Gurudatt, H. C. Tandon, *J. Taiwan Inst. Chem. Eng.* **2016**, *67*, 521.
[31] M. Faustin, A. Maciuk, P. Salvin, C. Roos, M. Lebrini, *Corr. Sci* **2015**, *92*, 287.
[32] E. B. Policarpi, A. Spinelli, *J. Taiwan Inst. Chem. Eng.* **2020**, *116*, 215.
[33] I.-M. Chung, R. Malathy, S.-H. Kim, K. Kalaiselvi, M. Prabakaran, M. Gopiraman, *J. Adhes. Sci. Technol.* **2020**, *34*, 1483.
[34] S. John, R. Jeevana, K. K. Aravindakshan, A. Joseph, *Egypt. J. Pet.* **2017**, *26*, 405.
[35] B. Nematian, S. A. A. Ramazani, M. Mahdavian, G. Bahlakeh, S. A. Haddadi, *Colloids Surf., A* **2020**, *601*, 125042.
[36] E. Ituen, O. Akaranta, A. James, S. Sun, *Sust. Mater. Technol.* **2017**, *11*, 12.
[37] Q. H. Dinh, T. Duong, N. P. Cam, *J. Chem.* **2021**. *2021*, 14.
[38] N. B. Iroha, N. A. Madueke, V. Mkpenie, B. T. Ogunyemi, L. A. Nnanna, S. Singh, E. D. Akpan, E. E. Ebenso, *J. Mol. Struct.* **2021**, *1227*, 129533.
[39] A. S. Ogunbadejo, O. E. Oladele, J. L. Olajide, O. E. Obolo, S. J. Olusegun, P. A. Olubambi, S. Aribo, *J. Bio- Tribo-Corros.* **2018**, *4*, 70.
[40] M. Manssouri, A. Laghchimi, A. Ansari, M. Znini, Z. Lakbaibi, Y. E. Ouadi, L. Majidi, *Mediterr. J. Chem.* **2020**, *10*, 253.
[41] Y. Koumya, R. Idouhli, O. Zakir, M. E. Khadiri, M. Zaki, J. E. Karroumi, A. Aityoub, A. Abourlfida, A. Benyaich, *Chem. Pap.* **2021**, *75*, 39.
[42] S. E. Hachani, Z. Necira, D. E. Mazouzi, N. Nebbache, *Acta Chim. Slov.* **2018**, *65*, 183.
[43] M. B. Radovanovic, Z. Z. Tasic, M. B. Petrovic Mihajlovic, A. T. Simonovic, M. M. Antonijevic, *Sci. Rep.* **2019**, *9*, 16081.
[44] A. Dehghani, G. Bahlakeh, B. Ramezanzadeh, M. Ramezanzadeh, *J. Mol. Liq.* **2019**, *279*, 603.

[45] N. Khedoudja, R. Cherif, A. Bezzar, L. Sail, A. Ait-Mokhtar, *Eur. J. Environ. Civil Eng.*, Published online **2021**, 14.
[46] S. Arul Xavier Stango, U. Vijayalakshmi, *J. Asian Ceram. Soc.* **2018**, *6*, 20.
[47] E. Ituen, O. Akaranta, A. James, *J. Taibah Univ. Sci.* **2017**, *11*, 788.
[48] P. Kannan, A. Varghese, K. Palanisamy, A. S. Abousalem, *J. Mol. Liq.* **2020**, *297*, 111855.
[49] P. Singh, V. Srivastava, M. A., Quraishi, *J. Mol. Liq.* **2016**, *216*, 164.
[50] A. Singh, K. R. Ansari, D. Singh Chauhan, M. A. Quraishi, S. Kaya, *Sust. Chem. Pharm.* **2020**, *16*, 100257.

How to cite this article: S. T., M. Dhayalan, J. R., R. Govindasamy, M. R. S. U., M. Ali Khan, M. Sillanpää, *Mater. Corros.* **2021**, 1–13.
https://doi.org/10.1002/maco.202112742